Neutron scattering studies of ordered gamma -ZrD

1994 J. Phys.: Condens. Matter 6 8977

(http://iopscience.iop.org/0953-8984/6/43/004)

J. Phys.: Condens. Matter 6 (1994) 8977–8988. Printed in the UK

Neutron scattering studies of ordered γ-ZrD

A I Kolesnikov†‡, A M Balagurov§, I O Bashkin†, A V Belushkin§‖, E G Ponyatovsky† and M Prager‡

† Institute of Solid State Physics of the Russian Academy of Sciences, 142432 Chernogolovka, Moscow District, Russia

‡ Institut für Festkörperforschung, Forschungszentrum Jülich KFA, D-52425 Jülich, Germany

§ Frank Laboratory of Neutron Physics, Joint Institute for Nuclear Research, 141980, Dubna, Moscow District, Russia

‖ Rutherford Appleton Laboratory, Chilton, Didcot, Oxon OX11 0QX, UK

Received 7 July 1994

Abstract. The crystal structure and the lattice dynamics of the ordered γ-ZrD phase were studied by means of neutron diffraction and inelastic neutron scattering (INS). It was found that the actual structure of the γ phase is orthorhombic, space group Cccm, rather than tetragonal as previously believed. The one-phonon deuterium optical band in the INS spectrum was observed at an energy transfer of 107 meV (with the main feature at 103.4 meV), which is higher than the deuterium vibrational energies for all other phases of the Zr–D system. Distinct features were also observed in the INS spectrum below the free multiphonon bands, which were explained as the bound multiphonon states.

1. Introduction

The phase diagram of the Zr–H system at atmospheric pressure is very similar to that of Ti–H [1, 2]. The equilibrium phases are solid solutions of hydrogen in α-Zr (the HCP metal sublattice) and in β-Zr (BCC), and deficient dihydrides δ-ZrH_{2-y} (hydrogen is randomly distributed on tetrahedral interstices of the FCC metal sublattice) and ε-ZrH_{2-y} with the FCT metal sublattice (axial ratio $c/a < 1$). The thermodynamic stability of monohydride γ-ZrH has recently been concluded from reversibility of the γ to $\alpha+\delta$ transformation [3, 4]. Sidhu and co-workers reported earlier [5] that hydrogen in the γ-ZrD was ordered on tetrahedral interstitial sites on alternate {110} planes of the FCT metal sublattice with a ratio $c/a = 1.081$.

A similar γ phase has also been found in the Ti–H samples after thermobaric [6–8] or thermal [9–11] treatments. Further x-ray and neutron diffraction experiments showed that the metal sublattice of γ-TiH was face-centred orthorhombic, FCO, and the crystal space group was Cccm [12–15]. The lattice parameters a and b differed by about 1%, but the axial ratio c/a was $\simeq 1.09$. Such a small orthorhombic distortion could not be detected with the resolution of conventional neutron diffractometers.

The dynamics of hydrogen in the α, β, δ and ε phases, and in the δ phase particularly, of the Zr–H(D) system has been the subject of numerous works [16–21], but the phonon spectrum of the ordered monohydride, γ-ZrH, has never been measured.

Recent inelastic neutron scattering (INS) experiments on γ-TiH(D) produced by a thermobaric treatment have shown the high anharmonicity of hydrogen (deuterium) vibrations [22–24]. Distinct peaks were observed in the INS spectra below the bands of two-phonon and three-phonon scattering. They were discussed in terms of bound

0953-8984/94/438977+12$19.50

multiphonons, biphonons and triphonons—new excitations which appear in the lattice dynamical description of systems with large anharmonicity. The effect of anharmonicity on the spectra of optical phonons and the nature of the bound phonons were the subject of theoretical and experimental (Raman and IR spectroscopy) works reviewed in [25]. However, optic investigations are limited to the long-wavelength part of the multiphonon spectra; γ-TiH(D) was the first hydride where both biphonons and triphonons were observed in the high-energy range using the INS technique. The origin of these features was related to the unique crystal structure of the γ phase [15, 22–24] where the H–H interaction is strong and essentially one-dimensional because the H–H distances along the c axis are reduced compared to those in the ab plane by a factor of $\sqrt{2}/1.09 \simeq 1.3$. A similar relation is valid in the case of γ-ZrH.

In the work described in this paper we studied the crystal structure of monodeuteride γ-ZrD using a time-of-flight neutron diffractometer. We found that it was not tetragonal, but orthorhombic, similar to γ-TiD. We then measured the INS spectrum of γ-ZrD and gained the first data on the fundamental deuterium modes and multiphonon bands in this monodeuteride. The data clearly show that bound multiphonon states actually occur in the γ-ZrD phonon spectrum, as was anticipated from the one-dimensional D–D interaction.

2. Experimental

To prepare the sample, a Zr ingot of 99.96 at.% purity was heated in a vacuum of $\sim 7 \times 10^{-3}$ Pa to 1070 K and allowed to absorb gaseous deuterium which was obtained by thermal decomposition of TiD_2. The deuterium content was determined from the weight gain, $x = D/Zr = 0.28 \pm 0.01$. It was confirmed by vacuum outgassing a part of the sample at 1170 K. A plate of size $23 \times 45 \times 3.3$ mm^3 was spark-cut from the $ZrD_{0.28}$ ingot and mechanically polished. Mechanical polishing was employed instead of etching in acids to avoid hydrogen contamination of the sample. The plate was then quenched in water from 923 K, well above the eutectoid temperature (823 K [1]), to 300 K and annealed in air at 450 K for about 140 hr. This thermal treatment has much in common with the ageing procedures [26, 27]. Only two phases, α and γ, were detected in this sample by x-rays.

Neutron diffraction patterns were obtained at room temperature using the time-of-flight Fourier diffractometer HRFD [28] at the IBR-2 pulsed reactor (Joint Institute for Nuclear Research, Dubna). We used it in high-resolution mode to obtain the lattice parameters and in medium-resolution mode to perform the Rietveld refinement of the diffraction spectrum.

The INS measurements were carried out at 30 K on the time-focused crystal analyser (TFXA) spectrometer [29] at the ISIS spallation neutron source of the Rutherford Appleton Laboratory, UK. Here, neutrons from a time-resolved white incident beam are scattered by the sample. Those neutrons emitted at an angle of $\simeq 135°$ with an energy of $\simeq 4$ meV pass an analyser consisting of a PG crystal and a Be filter and are recorded. An excellent resolution $\Delta\omega/\omega \leqslant 2\%$ was provided in the range of neutron energy transfer studied: 2–500 meV.

The measured spectrum was transformed to $S(Q, \omega)$ against energy transfer (meV) using standard programs, and then the background from an empty can in the cryostat was subtracted.

3. Neutron diffraction

The neutron diffraction data (figure 1, points) were treated using the multiphase profile Rietveld refinement program adapted for time-of-flight diffractometers [30]. A two-phase

state of the $ZrD_{0.28}$ sample, consisting of α and γ phases was assumed at the beginning. The differential curve between the experimental and calculated intensities, however, exhibited some peaks at positions close to the Bragg reflections from the δ phase. Therefore, the experimental data were finally treated assuming a three-phase state of the sample, α, γ and δ. The α and δ phases were fitted with space groups $P6_3/mmc$ (No 194) and $Fm3m$ (No 225), respectively. The deuterium content in the α phase (less than 0.001 at 300 K [1]) was neglected because the statistics of the spectrum was insufficient to determine this parameter.

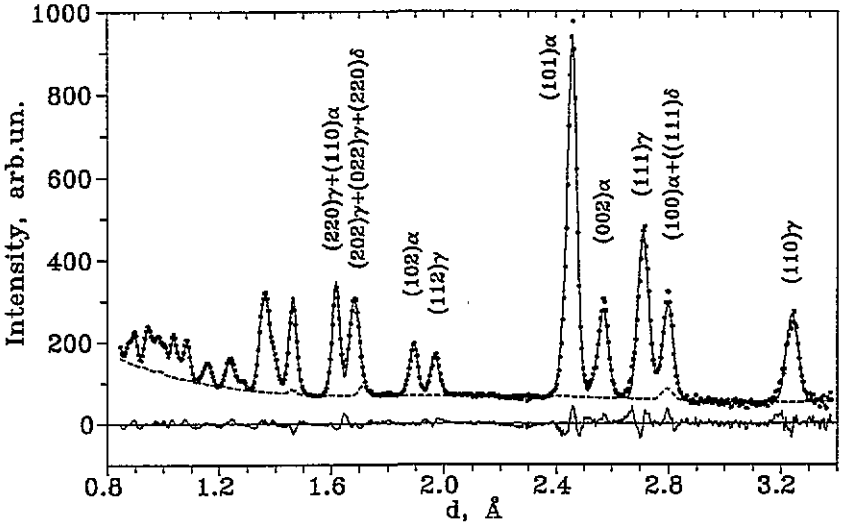

Figure 1. Neutron diffraction pattern of the $ZrD_{0.28}$ sample (points) measured at room temperature. Full curves represent the fit with a three-phase model ($\alpha+\gamma+\delta$) and the differential curve. The small amount of the δ phase detected by the Rietveld refinement is shown as a broken curve.

It was found from the high-resolution spectrum that the structure of the γ phase was FCO rather than FCT known from literature [1,5]. For example, the width of the (202) peak in the high-resolution spectrum was almost two times larger than that of neighbouring peaks. The FCO lattice parameters calculated from the high-resolution spectrum were used as the initial values for the Rietveld refinement, they were unaltered at the refinement within the experimental accuracy.

The results of the Rietveld analysis with R factors $R_w = 0.07$ and $R_p = 0.05$ are: (i) γ-ZrD_y: space group Cccm (no 66), $a = 4.549(1)$ Å, $b = 4.618(1)$ Å, $c = 4.965(1)$ Å, $y = 0.98(3)$, deuterium atoms occupying tetrahedral interstitial sites on alternate {110} planes; (ii) α-Zr: $a = 3.2332(4)$ Å, $c = 5.1466(10)$ Å; and (iii) δ-ZrD_y: $a = 4.842(5)$ Å, $y = 1.2(3)$ where the numbers in parentheses are estimated errors in the last digit.

The calculated lattice parameters of the α phase are close to other data [1]. The FCO structure of the γ phase with axial ratios of $b/a \simeq 1.015$ and $c/a \simeq 1.091$ is consistent with the crystal structure of the analogous phase, γ-TiD, studied recently [12–15]. The calculated lattice parameter of the δ phase is too high while the deuterium content is too low compared to earlier data (4.7803 Å, $y \simeq 1.62$ [1]). Due to a very small amount of this phase in the sample, a small grain size could possibly influence the structural parameters.

The low intensity of the Bragg peaks also explains why this phase was not detected by x-rays.

The results showed that the ratio of Zr atoms in the δ phase to those in the γ phase was less than 0.05, and the following phase relation was obtained for the sample at room temperature:

$$ZrD_{0.28} \Longleftrightarrow 0.718(\alpha\text{-}ZrD_{0.001}) + 0.269(\gamma\text{-}ZrD_{0.98}) + 0.013(\delta\text{-}ZrD_{1.2}). \quad (1)$$

It is worth noting that very broad diffraction peaks (twice as wide as usual) were characteristic of all phases, and the reflections broadened as the d spacings increased. This indicates strain gradients in the sample, and could be expected from internal stress due to thermal treatment. Furthermore, defects at the phase boundaries could also contribute to the peak broadening.

4. Inelastic neutron scattering

The deuterium content in α-Zr is negligible at $T = 30\,K$ [1]. Therefore, the α phase contributes to the INS spectrum only in the range of lattice vibrations. We can also neglect the dihydride δ-phase contribution to the INS spectrum because of its small content.

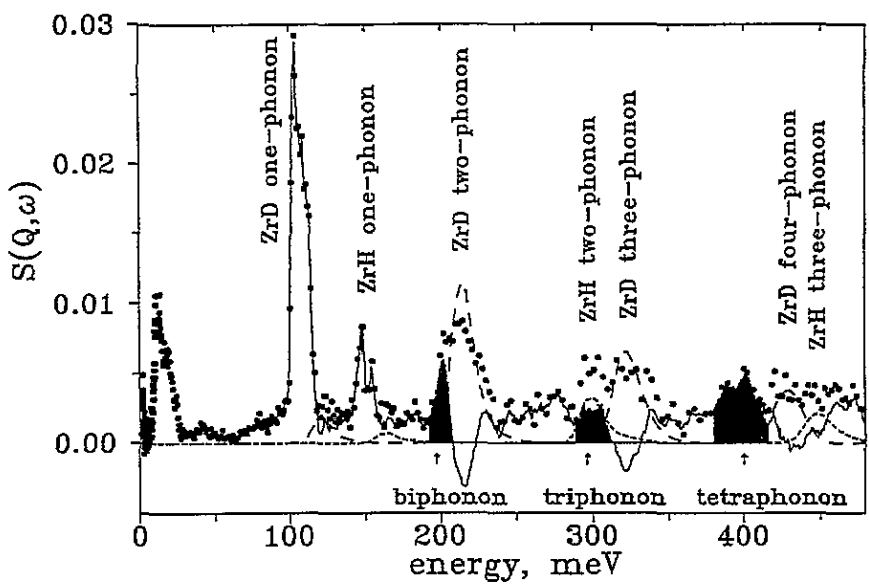

Figure 2. The INS spectrum $S(Q,\omega)$ of $(\alpha+\gamma)$-$ZrD_{0.28}$ at 30 K (points). The calculated multiphonon contributions for the deuterium atoms are shown by the long-dash broken curve. The short-dash broken curve represents the hydrogen multiphonon contribution. The full curve represents the difference between the experimental data and the calculated multiphonon spectra. The black areas are attributed to bound multiphonon states.

The experimental INS spectrum for the $ZrD_{0.28}$ sample, $S(Q,\omega)$, is shown as points in figure 2. The low-energy range of the spectrum, 0–30 meV, is associated with vibrations of heavy Zr atoms in α and γ phases (lattice vibrations); the next interval, 95–120 meV,

represents deuterium optical modes; the range above 170 meV is related to multiphonon processes of neutron scattering on deuterium atoms.

The spectrum in figure 2 also includes a split peak around 150 meV, which is due to a small content of hydrogen in the sample. This assignment is confirmed by the energy ratio between this peak and the deuterium optical peak, which is close to $\sqrt{m_D/m_H} = \sqrt{2}$. Here m_D and m_H are the deuterium and hydrogen atomic masses. The amount of hydrogen impurity is 0.9%, as estimated from the ratio of peak intensities. A similar contamination of the γ-TiD sample used in a previous study [23] is an indication of the hydrogen impurities in our source of deuterium, TiD_2.

4.1. Multiphonon scattering contributions

Contributions from multiphonon neutron scattering were calculated in the harmonic isotropic approximation up to four-phonon processes by means of an iterative technique using convolution of the one-phonon spectrum [22, 31]. Experimental data in the energy range of the lattice and deuterium optical phonons, 2–120 meV, were used in the first step as a one-phonon spectrum of deuterium vibrations. In the range of lattice vibrations the intensity of the spectrum was reduced by a factor of 13.7 in order to take into account contributions from deuterium atoms in the γ phase only. This factor was deduced from the phase relation (1) and from the ratio of integrated partial intensities $S(Q, \omega)$ for deuterium and zirconium atoms. The model calculations of the γ-ZrD lattice dynamics (section 4.4) demonstrated that this ratio is equal to 0.29 in the range of lattice vibrations. Assuming the same neutron scattering on Zr atoms in α and γ phases we get a value of 1/13.7 for contributions of D atoms to the lattice range.

The calculated multiphonon contributions were subtracted from the experimental spectrum, and the difference was taken as a new one-phonon spectrum for the second and further steps of the calculation. Convergence was reached in three iterations.

A similar iterative procedure was carried out to calculate the multiphonon neutron scattering on hydrogen atoms. In this case, the spectrum in the energy range 140—160 meV was assumed to be due to the one-phonon hydrogen optical modes.

The calculated spectra for multiphonon neutron scattering on deuterium and hydrogen atoms are plotted in figure 2 in long- and short-dash broken curves, respectively. The full curve represents the difference between the experimental spectrum and the calculated multiphonon contributions.

4.2. Lattice vibrations

Figure 3 shows the generalized vibrational density of states $\Theta(\omega)$ in the range 0–30 meV (points) calculated from the experimental $S(Q, \omega)$ spectrum according to

$$\Theta(\omega) = \frac{\exp(2\mathrm{DW})S(Q,\omega)\omega}{Q^2[n(\omega)+1]} \tag{2}$$

where ω and Q are the neutron energy and the momentum transfer, respectively, DW is the Debye–Waller factor and $n(\omega)$ is the Bose factor. The spectrum is normalized to unity in the range 0–26 meV.

Neutron scattering intensities in the lattice region of the INS spectrum are mainly determined by Zr vibrations. A calculation of the γ-ZrD lattice dynamics (section 4.4) showed that the γ phase contributed only 33% to the integrated intensity in the lattice range. This means that 67% of the integrated intensity was due to neutron scattering on

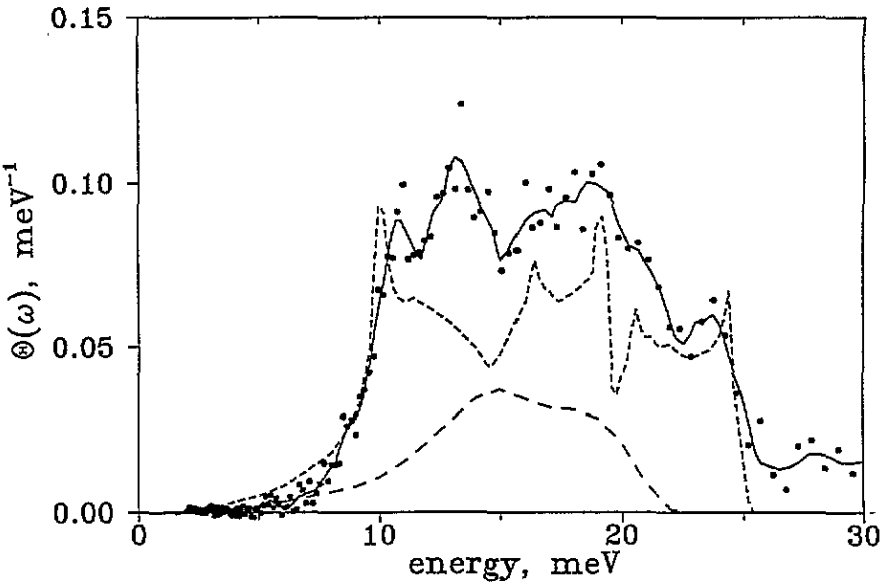

Figure 3. Generalized vibrational densities of states $\Theta(\omega)$ of $(\alpha+\gamma)$-$ZrD_{0.28}$ in the range of lattice vibrations. Experimental points were calculated from the measured $S(Q,\omega)$ spectrum on the basis of (2). The smoothed spectrum is shown as a full curve. The calculated densities of phonon states of α-Zr [32] and γ-ZrD (present work) are shown as short- and long-dash broken curves, respectively. Two features were fitted for γ-ZrD: the peak at 14 meV and the spectrum cutoff at 22 meV.

zirconium vibrations in the α phase. The spectrum in figure 3 should therefore be compared to that of α-Zr (see below).

Stassis and co-workers [32] calculated the density of phonon states in α-Zr using the room-temperature values of force constants determined from the experimental phonon dispersion curves. Their spectrum is normalized in figure 3 to the value of 0.67 (the short-dash broken curve). Comparison of their experimental data at helium and room temperatures [32] shows that the first peak at 10 meV (TA and lower TO modes) and the last peak at 24 meV (LO type) displaced by 1–2 meV to higher and lower energies, respectively, on cooling to 5.5 K. Therefore, the prominent features at 11, 16.5, 18.5, 21 and 23.5 meV of the present spectrum can be attributed to the α-Zr phonon spectrum. But the strong peak at 14 meV should be associated with the Zr vibrations in γ-ZrD. This peak, as well as the cutoff of the spectrum at 22 meV, represent two features in the range of the lattice modes described by the model calculations of γ-ZrD (see below; long-dash broken curve in figure 3).

4.3. Deuterium optical modes

The band at 107 meV is related to the deuterium optical modes. Figure 4 displays a well resolved structure of this band. It is best fitted with three Gaussians (short-dash broken curve). For a quantitative comparison with other zirconium hydrides, the band was also described by a sum of two Gaussians. The parameters of the Gaussians are listed in table 1. Since other related INS experiments were carried out mainly on hydrides, table 1 also includes the values of $\omega_i\sqrt{2}$ which give the energies of hydrogen optical modes in γ-ZrH estimated in a harmonic approximation.

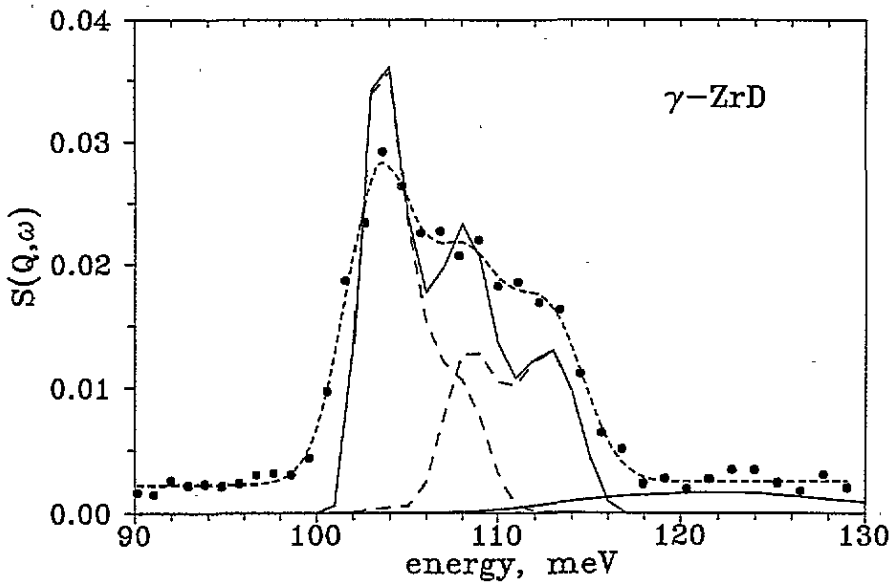

Figure 4. The spectrum $S(Q,\omega)$ for γ-ZrD in the range of the deuterium optical modes. Shown are experimental points, a three-Gaussian fit (short-dash broken curve), multiphonon contributions (lower full curve) and the calculated one-phonon spectrum (full curve). The calculated spectrum was convoluted with the resolution function for TFXA spectrometer (a triangle with a width at half maximum of $\Delta E = 0.02\omega$). The contributions to the spectrum from vibrations of the D atoms in the *ab* plane (the left peak) and along the *c* axis (the split peak at the right side) are shown as long-dash broken curves.

Table 1. Peak positions ω_i (meV), full widths at half-maximum δ_i (meV) and peak amplitudes H_i (arbitrary units) for Gaussians describing the optical band in the INS spectrum of γ-ZrD. The line $\omega_i\sqrt{2}$ represents the energies of hydrogen optical peaks estimated from the present data on γ-ZrD in the harmonic approximation. Also presented are parameters of the hydrogen impurity peak.

	γ-ZrD			γ-ZrD		γ-ZrH	
	$i=1$	$i=2$	$i=3$	$i=1$	$i=2$	$i=1$	$i=2$
ω_i	103.4	108.0	112.7	103.4	109.4	147.2	154.3
$\omega_i\sqrt{2}$	146.2	152.7	159.4	146.2	154.7		
δ_i	4.4	4.9	4.8	4.4	9.4	5.3	2.8
H_i	0.37	0.27	0.20	0.30	0.29	0.084	0.056

The following data on hydrogen optical modes were obtained in earlier experiments on Zr–H phases.

(i) α-ZrH_y, $y = 0.03$–0.05, shows a very broad peak at 143–144 meV with the full width at half-maximum (FWHM) equal to 47 meV [16, 21].

(ii) The δ phase of ZrH_y, $0.54 \leqslant y \leqslant 1.56$, has a broad peak at energies of 130–140 meV with FWHM ranging from 15–37 meV [17, 18, 33–35].

iii) ε-ZrH_y, $1.9 \leqslant y \leqslant 2$, shows a split peak with maxima at energies 136–138 meV and 143–145 meV and a high-energy shoulder at 154 meV [17–19]. The shoulder was explained by multiphonon processes which combine optical and acoustic vibrations [19].

It is evident that the energy of the optical peak in the γ phase is higher than in any other phase of the Zr–H system. This correlates with the shortest hydrogen-to-metal nearest-neighbour distances in the γ phase, $R_{Zr-D(H)} = 2.041$ Å, compared to 2.070 and 2.082 Å in the δ and ε phases, respectively. If a $1/R^n$ dependence is assumed for the energy of hydrogen vibrations, then we obtain $n \approx 4$. This value is rather large compared to $n \approx 1$–2 for hydrides of other metals [36–40].

Quite another dependence of the optical frequency on hydrogen-to-metal distance is observed in the α phase compared to the γ phase. The distance in the α phase, $R_{Zr-D(H)} = 2.011$ Å at 873 K [1] is less, but the hydrogen vibrations are softer than in the γ phase. The local relaxation of the lattice in the α phase due to the low hydrogen content can explain this behaviour only partially.

Thus, this behaviour is indicative of a steeper potential for hydrogen atoms in the γ phase compared to any other Zr–H phase.

4.4. Model calculations for γ-ZrD

There are several models for calculating the lattice dynamics of metal hydrides. A simple model of localized deuterium vibrations, which takes into account only the longitudinal Zr–D forces, results in a deuterium optical band in the INS spectrum of γ-ZrD, which is well resolved into two lines. The lower-energy line is doubly degenerate, and the other one is non-degenerate. This simple model contradicts to the experimental data. Dispersion of the deuterium optical modes due to the D–D interaction was therefore taken into account. For this purpose, the Born–von Kármán model was applied to describe the experimental phonon spectrum of γ-ZrD.

Under the usual assumption of central forces, the number of fitting parameters is two for each interacting pair, namely the longitudinal (L) and transverse (T) force constants. Interactions between the nearest D–Zr, Zr–Zr and D–D (at a distance of $c/2$ along the crystal c-axis) neighbours were expected to be dominant, but the second and third D–D neighbours at D–D distances $\sqrt{a^2 + b^2}/2$ in the ab plane and $\sqrt{a^2 + b^2 + c^2}/2$ in the (111) direction, respectively, were also involved. The UNISOFT program [41] was used for the calculation.

Fitting the spectrum in the range of lattice vibrations was complicated because of the large contribution from α-Zr. Thus, fitting of the two Zr–Zr force constants in the γ phase was limited to reproducing only the peak near 14 meV and the cutoff of the lattice modes near 22 meV. Varying these parameters had no effect on the deuterium optical modes. Thus, the main adjustable parameters for this model were the force constants of the Zr–D and D–D interaction. The former determined the average energy of D vibrations, and the latter was responsible for the shape of the peak due to dispersion of the optical modes.

The weighted densities of phonon states were obtained according to

$$G_i(\omega) = \frac{1}{3Nm_i} \sum_{j,q} |e(i|qj)|^2 \delta\big(\omega - \omega_j(q)\big) \tag{3}$$

where $\omega_j(q)$ and $e(i|qj)$ are eigenvalues and eigenvectors of the dynamical matrix corresponding to the phonon state qj, and m_i is the mass of atom i. The summation runs over N=1728 points in q space uniformly distributed over the reduced Brillouin zone. To compare with the experimental spectrum, we transformed the calculated data to

$$S(Q, \omega) = \frac{\hbar Q^2}{6\omega} \sum_i \exp(-Q^2\langle u_i^2\rangle)\sigma_i G_i(\omega)[n(\omega) + 1] \tag{4}$$

where σ_i is the neutron scattering cross section of atom i, and $\langle u_i^2 \rangle$ is the mean square amplitude of displacement of atom i averaged over all modes. The $\langle u_i^2 \rangle$ values were calculated from

$$\langle u_i^2 \rangle = \int \frac{\hbar}{12\omega} G_i(\omega)[2n(\omega)+1]\, d\omega. \tag{5}$$

Table 2. Values of the longitudinal (L) and transverse (T) force constants (in $N m^{-1}$) of the Born–von Kármán model adapted to fit the experimental spectrum.

	First neighbour		Second neighbour		Third neighbour	
	L	T	L	T	L	T
D–D	3.0	1.5	−1.5	0.	1.0	0.
Zr–D	31.4	15.7				
Zr–Zr	8.0	0.				

The calculated $S(Q, \omega)$ spectrum was fitted to the experimental one by a trial-and-error method. The force constants finally obtained are listed in table 2. The results of the fit are presented in figure 4. The calculated data describe the experimental spectrum fairly well. The contributions to the spectrum from D atoms vibrating in the *ab* plane (left peak) and along the *c* axis (split peak at the right) are shown as long-dash broken curves. Note the large dispersion of the peaks due to the D–D interaction.

It follows from the model calculations that the ratio of the integrated intensity of the $S(Q, \omega)$ spectrum in the range of lattice vibrations to the integrated intensity of the optical peak is 0.073. The ratio of the contributions to the lattice part of the spectrum from D and Zr atoms in the γ phase is equal to 0.29. Further simple estimates show that the contribution from α-Zr, the other phase in the sample, to the experimental spectrum in the range of the lattice vibrations is about 67%. These values were used above in calculating the multiphonon scattering and in the analysis of the lattice vibrations (sections 4.1 and 4.2).

4.5. Hydrogen optical peak

The small hydrogen impurity in the sample allowed some estimates of the isotope effect. Parameters of the two Gaussians fitting the hydrogen optical band are listed in table 1. The derived energy positions and those estimated from the deuterium optical band (also fitted with two Gaussians) agree well within the experimental resolution.

A model calculation of the γ-ZrH phonon spectrum was then performed using the force constants obtained for γ-ZrD. However, the calculated $S(Q, \omega)$ spectrum was in poor agreement with the experimental one. This discrepancy could be due to the low content of H atoms in the sample. Therefore, it is likely that hydrogen is dissolved in the deuteride as an isotopic impurity rather than as precipitated grains of γ-ZrH. In this case, hydrogen vibrations would be better approximated by local oscillators than by optical phonon modes. As was discussed at the beginning of section 4.4, localized vibrations of hydrogen in the γ phase should result in a well resolved two-peak optical band with the intensity ratio of the peaks $I_1/I_2 = 2$ and $\omega_1 < \omega_2$. The experimental band at 147–154 meV in figure 2 is in agreement with this estimate.

The broadening of the hydrogen optical peaks, δ_i, and their shift from the harmonic position in the vibrational spectrum were estimated as contributions of the mass disorder

(see [42, 43]) in the γ-$ZrD_{0.991}H_{0.009}$ sample. The calculated energy shift is less than 0.1 meV. This is negligible compared to the spectrometer resolution. The estimated broadening of the peaks is 4.7 and 2.6 meV, which is in good accord with the experimental data (table 1).

4.6. Bound multiphonon states at high energies

The multiphonon spectrum (long-dash broken curve in figure 2) calculated in the harmonic approximation (section 4.1) accurately describes the main part of the experimental data. However, some strong features could not be attributed within the harmonic approximation. They are clearly displayed in the difference between the experimental spectrum and the calculated multiphonon contributions given by the full curve in figure 2. Each feature combines a peak or a band of excess intensity well below any harmonic estimate (black regions in figure 2) and some deficit in the integrated intensity of the harmonic multiphonon bands. The areas of the excess peaks and intensity deficiencies are comparable for the two- and three-phonon processes.

The correlation is less evident for the four-phonon band because the multiphonon calculations were carried out only up to four-phonon contributions, and thus no lattice vibrations were taken into account for the deuterium optical four-phonon band.

The energies and FWHM (in parentheses) characterizing the anharmonic peaks are $E_2 = 201$ (7) and $E_3 = 299$ (15) meV. The band around 396 meV has two maxima, which we ascribe to a superposition of the anharmonic peak at $E_4 = 387(15)$ meV and the combined excitations of $\omega_1 + E_3$ and $2E_2$ (both are at an energy 402(15) meV).

The nature of the anharmonic peaks can be treated in terms of the strong interaction between the optical phonons. Bound multiphonon states (biphonons and triphonons), which do not occur in a harmonic crystal, can be created due to the strong phonon interaction [25, 44, 45]. Such a quasi-particle moves through a crystal as a whole and has a definite energy and wavevector, similar to a phonon. The D–D interaction in γ-ZrD has a one-dimensional character, and it was shown in [25, 44] that in one- or two-dimensional anharmonic systems bound multiphonon states are more likely to exist. The energies of these bound phonon states are defined by the simple expressions [44, 45]

$$E_2 = 2\omega - 2A \qquad E_3 = 3\omega - 6(A + \tilde{A}) \tag{6}$$

where ω is the energy of the optic phonons, and A and $\tilde{A}$ are the anharmonicity parameters which determine the strength of the two- and three-phonon interaction, respectively.

The anharmonicity parameters for γ-ZrD are $A \approx 3$ meV and $\tilde{A} \approx -1$ meV. These values are about half as large as those found earlier for γ-TiD [23].

It is interesting to note that the anharmonic peak at $E_4 = 387$ meV is distinctly separated from the band of free four-phonon states and can be considered as tetraphonon excitations. This would be the first observation of bound four-phonon states in metal hydrides.

The present results are in good agreement with earlier data on γ phases of TiH and TiD. The validity of assignments of all peaks in the γ-ZrD INS spectrum is also confirmed by the recent INS study of γ-ZrH, where measurements were carried out with better statistics.

5. Conclusions and summary

The detailed neutron diffraction study shows that the γ-ZrD crystal structure is characterized by the space group Cccm, where deuterium atoms occupy tetrahedral interstitial sites on alternate {110} planes of the FCO rather than earlier stated FCT metal sublattice.

The fundamental band of deuterium vibrations was observed by INS at an energy of 107 meV (the main feature at 103.4 meV), which is rather high compared to other phases of the Zr–H system. The experimental deuterium optical band was accurately described by means of the Born–von Kármán model calculations of the γ-ZrD phonon spectrum, which elucidated the dispersion of the optical phonon modes.

Anharmonic peaks were observed in the high-energy range of the spectrum below the free multiphonon bands. They were attributed to the bound multiphonon states (biphonon, triphonon and tetraphonon excitations).

Acknowledgments

The authors thank Professor V G Glebovsky of the ISSP Russian Academy of Sciences, who provided high-purity zirconium. Special thanks are due to Dr G Eckold (Technische Hochschule, Aachen) for providing the UNISOFT program. We are grateful to the SERC for access to the ISIS pulsed neutron source. One of us (AIK) thanks the Alexander von Humboldt Foundation for the research grant. The research described in this paper was made possible in part by Grant from the International Science Foundation No. REP000 and by Grant of Russian Ministry of Science No. 93–02–2530.

References

[1] Zuzek E, Abriata J P, San-Martin A and Manchester F D 1990 *Bull. Alloy Phase Diagrams* **11** 385–95, 2078–80
[2] San-Martin A and Manchester F D 1987 *Bull. Alloy Phase Diagrams* **8** 30–42, 81–2
[3] Bashkin I O, Malyshev V Yu and Myshlyaev M M 1992 *Sov. Phys.–Solid State* **34** 1182–4
[4] Bashkin I O, Malyshev V Yu, Ponyatovskii E G 1993 *Z. Phys. Chem.* **179** 307–17
[5] Sidhu S S, Satya Murthy N S, Campos F P and Zauberis D D 1963 *Adv. Chem. Ser.* **39** 87–98
[6] Bashkin I O 1989 *Z. Phys. Chem.* **163** 469–78
[7] Ponyatovsky E G and Bashkin I O 1985 *Z. Phys. Chem.* **146** 137–57
[8] Kolesnikov A I, Monkenbush M, Prager M, Bashkin I O, Malyshev V Yu and Ponyatovskii E G 1989 *Z. Phys. Chem.* **163** 709–14
[9] Numakura H and Koiwa M 1984 *Acta Metall.* **32** 1799–807
[10] Woo O T, Weatherly G C, Coleman C E and Gilbert R W 1985 *Acta Metall.* **33** 1897–906
[11] Bourret A, Lasalmonie A and Naka S 1986 *Scr. Metall.* **20** 861–6
[12] Numakura H, Koiwa M, Asano H and Izumi F 1988 *Acta Metall.* **36** 2267–73
[13] Mogilyanskii D N, Bashkin I O, Degtyareva V F, Malyshev V Yu and Ponyatovskii E G 1990 *Sov. Phys.–Solid State* **32** 1039–41
[14] Balagurov A M, Bashkin I O, Kolesnikov A I, Malyshev V Yu, Mironova G M, Ponyatovskii E G and Fedotov V K 1991 *Sov. Phys.–Solid State* **33** 711–4
[15] Kolesnikov A I, Balagurov A M, Bashkin I O, Fedotov V K, Malyshev V Yu, Mironova G M and Ponyatovsky E G 1993 *J. Phys.: Condens. Matter* **5** 5045–58
[16] Khoda-Bakhsh R and Ross D K 1982 *J. Phys. F: Met. Phys.* **12** 15–24
[17] Ikeda S and Watanabe N 1983 *Physica* B **120** 131–5
[18] Couch J G, Harling O K and Clune L C 1971 *Phys. Rev.* B **4** 2675–81
[19] Tomkinson J, Penfold J and Robertson S T 1989 *Rutherford Appleton Laboratory Internal Report* RAL-89-074
[20] Semenov V A and Lisichkin Yu V 1982 *Sov. Phys.–Solid State* **24** 2037–41
[21] Hempelmann R, Richter D and Stritzker B 1982 *J. Phys. F: Met. Phys.* **12** 79–86
[22] Kolesnikov A I, Prager M, Tomkinson J, Bashkin I O, Malyshev V Yu and Ponyatovskii E G 1991 *J. Phys.: Condens. Matter* **3** 5927–36
[23] Kolesnikov A I, Bashkin I O, Malyshev V Yu, Ponyatovsky E G, Prager M and Tomkinson J 1992 *Physica* B **180&181** 284–6

[24] Bashkin I O, Kolesnikov A I, Malyshev V Yu, Ponyatovsky E G, Prager M and Tomkinson J 1993 Z. *Phys. Chem.* **179** 335–42
[25] Agranovich V M and Lalov I I 1985 *Sov. Phys.–Usp.* **28** 484–505
[26] Mishra S, Sivaramakrishnan K S, Asundi M K 1972/73 *J. Nucl. Mater.* **45** 235–44
[27] Solodinin A M, Boyko E B and Andrievskii R A 1978 *Russ. Metall.* **1** 178–82
[28] Balagurov A M, 1991 *Physica* B **174** 542–5
[29] Penfold J and Tomkinson J 1986 *Rutherford Appleton Laboratory Internal Report* RAL-86-019
[30] Balagurov A M, Beskrovnyi A I, Popa N and Sangaa D 1987 *Communication of the Joint Institute for Nuclear Research* P14-87-744 (Dubna: JINR)
[31] Kolesnikov A I, Natkaniec I, Antonov V E, Belash I T, Fedotov V K, Krawczyk J, Mayer J and Ponyatovsky E G 1991 *Physica* B **174** 257–61
[32] Stassis C, Zarestky J, Arch D, McMasters O D and Harmon B N 1978 *Phys. Rev.* B **18** 2632–42
[33] Pelah I, Eisenhauter C M, Hughes D J and Palevsky H 1957 *Phys. Rev.* **108** 1091–2
[34] Andresen A, McReynolds A W, Nelkin M, Rosenbluth M and Whittemore W 1957 *Phys. Rev.* **108** 1092–3
[35] Pan S S and Webb F J 1965 *Nucl. Sci. Eng.* **23** 194–7
[36] Ross D K, Martin P F, Oates W A and Khoda Bakhsh R 1979 Z. *Phys. Chem.* **114** 221–30
[37] Sugimoto H and Fukai Y 1982 *J. Phys. Soc. Japan* **51** 2554–61
[38] Fukai Y and Sugimoto H 1981 *J. Phys. F: Met. Phys.* **11** L137–9
[39] Rush J J, Udovic T J, Hempelmann R, Richter D and Driesen G 1989 *J. Phys.: Condens. Matter* **1** 1061–70
[40] Hempelmann R, Richter D, Hartmann O, Karlsson E and Wäppling R 1989 *J. Chem. Phys.* **90** 1935–49
[41] Eckold G, Stein-Arsic M and Weber H-J 1986 *UNISOFT—A Program Package for Lattice-Dynamical Calculations: User Manual* (Jülich: IFF KFA) Jül-Spez-366
[42] Cardona M, Etchegoin P, Fuchs H D and Molinàs-Mata P 1993 *J. Phys.: Condens. Matter* **5** A61–72
[43] Fuchs H D, Grein C H, Devlin R I, Kuhl J and Cardona M 1991 *Phys. Rev.* B **44** 8633–42
[44] Agranovich V M, Dubovskii O A and Orlov A V 1986 *Phys. Lett.* **119A** 83–8
[45] Agranovich V M and Dubovskii O A 1986 *Int. Rev. Phys. Chem.* **5** 93–101